The chemical effects of CO_2 addition to methane on aromatic chemistry

M. Fischer[1] , X. Jiang

Engineering Department, Lancaster University, Lancaster LA1 4YR, UK.

Keywords:
Soot, PAH, Modeling, Chemical kinetics, Biogas, Bio-syngas

Abstract

This numerical study concerns the effect of CO_2 addition to CH_4 on aromatic chemistry. In the absence of any thermodynamical effects, *purely kinetic* factors cause increases in the amount of carbon dioxide to decrease benzene mole fraction. The reaction $H + CO_2 \rightleftharpoons OH + CO$ proved very important. Simulations under adiabatic conditions shows that raising the concentration of CO_2 leads to an *increase* in A_1 mole fractions. This is caused by CO_2 addition making the combustion less efficient, so that both the temperatures and the concentrations of the OH radical are lower than for pure methane. We also discovered that the CO_2 *kinetics* reduces the amount of benzene under isothermal conditions whereas it increases it under adiabatic conditions. Finally, we found that CO_2 addition to *benzene* has negligible kinetic effects on aromatic hydrocarbons, radicals and even CO. Overall, our study shows that the kinetic effects of carbon dioxide in biogas can be highly complex, non-linear and counter-intuitive.

1. Introduction

Owing to the dire repercussions that man-made global warming are likely to have on our environment, health, economies, and societies, most studies aimed at assessing the sustainability of potential renewable fuels have tended to focus on Greenhouse Gases (GHG) [1, 2]. Studies investigating the formation of other pollutants less directly relevant to climate change during the combustion of putative sustainable fuels tend to be rather rare in comparison.

Among potentially sustainable fuels, biogas and bio-syngas and related blends are attracting an increasing interest among researchers and practitioners alike [3–5]. Biogas is formed via the anaerobic degradation of organic material [6] and is essentially constituted of methane and carbon dioxide. Syngas (synthesis gas) is basically a blend of carbon

---

[1] Corresponding Author: Marc Fischer.
E-mail address: m.fischer@lancaster.ac.uk
Telephone number: +44 1524 594645.

monoxide and hydrogen which is employed for synthesising diverse products [7]. The gasification of coal is most often utilised for its production. Bio-syngas is a form of synthesis gas which is formed through the thermal gasification of biomass. It is made up of CO, CO_2, CH_4 and H_2 and is considered to be a cleaner fuel than biogas due to its higher hydrogen content [8]. In three recent publications [9–11], we investigated the chemical kinetics of CH_4 - CO - H_2 - CO_2 fuel mixtures by using ignition delay times measured inside shock tubes.

In the current work, we want to turn our attention to the effects of the use of these fuels on the formation of the precursors of soot, the PAH. Along with CO, CO_2 and NOx, soot is one of the most important and preoccupying pollutants emitted in exhaust fumes [12, 13]. It stems from the incomplete combustion of fuel under rich conditions. These prevail when, for instance, too high amounts of fuel have been introduced into a combustion chamber or the mixing with the oxidant was insufficient [14]. In the industrial world, millions tonnes of soot are produced on a yearly basis, mainly for the production of tires or coloured figments such as black figments used for printing [15]. Sooting flames are characterised by a yellowish glow that can greatly contribute to heat transfer in industrial burners, thereby raising their efficiency [16]. Nevertheless, soot production also naturally increases the number of airborne particles hovering in the lower and upper atmosphere [17]. Upon inhalation, soot particles can penetrate into lungs and reach, according to their size, different depths [18]. The farther they go, the harder they can be driven out of the lungs or decomposed through natural purification processes [19]. Very small particles can go down to the alveoles and get absorbed by cells where they can cause irritations and even lung cancers [20]. Aside from causing damages to human health, soot has also a negative influence on the environment. Thus, soot particles relatively close to the ground play a role in the emergence of smog [21]. Airborne soot particles reduces the reflection of the sun which is a further cause of global warming [22]. They could also potentially contribute to the depletion of the ozone layer [23].

Consequently, when evaluating the local and global effects of allegedly renewable fuels, more studies need to be devoted to the effects of their use in terms of soot production and balance and the related aromatic chemistry. The purpose of our numerical investigation was to reach a better understanding of the **chemical kinetic** role of carbon dioxide in soot formation by considering *homogeneous time-dependent* systems where chemical kinetics and thermodynamics can be uncoupled from other phenomena (such as diffusion, turbulent mixing, convection and so on and so forth) whose overlap can severely hamper the identification of empirical trends, the attribution of causes to observations and the development of predictive models.

This article is organised as follows. Section 2 offers a review of the chemical kinetics of soot formation, especially in relation to the combustion of CH_4-CO_2 blends. Section 3 lays out the methodology used to estimate the effects of CO_2 addition on the formation of soot and its precursors. Section 4 compares the performance of five reaction mechanisms aimed at simulating soot precursors with respect to the homogeneous combustion of biogas, bio-syngas and related mixtures. Section 5 investigates numerically the **purely chemical** effects of CO_2 (25%, 50%, and 75%) addition to methane under isothermal conditions. In section 6, the effects of carbon dioxide addition to CH_4 are numerically studied under adiabatic conditions. In section 7, the direct addition of CO_2 to A_1 is investigated with respect to aromatic chemistry. Finally, section 8 provides readers with the conclusion, the outlook and recommended experimental studies to be carried out in the future.

2. Existing literature related to soot formation and CO_2

Historically, the formation of carbonaceous particulate matter during the pyrolysis and rich oxidation of fuels has been attributed to either the formation and growth of poly-acetylene or polyyne ([24]) or to the appearance and growth of polycyclic aromatic hydrocarbons ([14, 25]) which contain at least two benzene-type rings. Over the last years and decades, numerous experimental and theoretical results ([26–29]) have revealed that soot is almost exclusively formed through the aromatic pathway whereas the polyacetylene route could at most only play a minor role by leading to the formation of specific PAH. Readers interested in the general aspects of soot formation are referred to the works of McEnally and Pfefferle [30], Richter et al. [25], and Bockhorn [31]. Of greatest importance to the present study is the *chemical* effect of the addition of CO_2 to methane (which may be used to represent various compositions of bio-syngas and biogas [9], [10]) upon aromatic chemistry.

Several studies indicate that the presence of carbon dioxide in biogas leads to a more limited formation of soot as compared to pure methane. Samanta et al. [32] performed a numerical analysis of methane-air laminar nonpremixed flames with different levels of dilution in CO_2. They found out that increases in the original carbon dioxide mole fraction go hand in hand with a decrease in soot and NO formation. Charest et al. [33] studied laminar diffusion biogas flames with various amounts of CO_2 present in the fuel. They identified a soot suppression effect varying linearly with the concentration of carbon dioxide. Whilst they do not rule out reactions between CO_2 and other species, they explained this phenomenon in terms of the effects of *dilution* on chemical reaction rates. Apart from these two studies, there does not seem to be, to the best of our knowledge, any further investigations into the effects of carbon dioxide addition on the sooting tendency of flames having methane as a fuel.

The effects of CO_2 addition on the sooting tendencies of C_2H_4 have been extensively studied by a number of authors who drew partially conflicting conclusions from their results. In an experimental study involving ethylene spherical diffusion flames in micro-gravity, Berhan et al. [34] noticed that soot formation is inhibited by CO_2 addition although they did not analyse the underlying causes. Kailasanathan et al. [35] investigated ethylene laminar diffusion flames. They discovered that among four diluents (Argon, helium, nitrogen, and carbon dioxide), CO_2 is the one leading to the highest suppression of soot. This effect was largely attributed to differences in the thermal diffusivities of the four species, and it is not clear whether or not chemical reactions undergone by CO_2 also played a role in that result. Liu et al. [36] also considered ethylene diffusion flames. They found that the chemical suppression of soot formation can be traced back to the elementary steps $CO_2 + H \rightarrow CO + OH$ and $CO_2 + CH \rightarrow HCO + CO$. The higher concentration of oxidising radicals, in turn, leads to lower concentrations of acetylene (thereby limiting the extent of soot inception) and a stronger oxidation of the soot particles themselves. Mancarella et al. [37] studied CO_2 addition to fuel-rich premixed ethylene flames. According to their numerical analysis, the reduction in the formation of soot is mainly due to the oxidation of soot particles and their precursors PAH by hydroxyl radicals formed via the reaction $CO_2 + H \rightarrow CO + OH$. Annunziata et al. [38] investigated ethylene laminar counter-flow diffusion flames where a certain proportion of the inert carrier gas Argon had been replaced by varying amounts of carbon dioxide. They attributed the decrease in soot concentration mainly to thermal effects stemming from the thermodynamic properties of gaseous CO_2 when compared to those of Ar. Guo et al. [39] performed a numerical study involving ethylene diffusion flames. They discovered that the reduced concentration of the hydrogen radical (via $CO_2 + H \rightarrow CO + OH$) suppresses soot inception and lowers surface growth rates whereas the oxidation of the particles is only very weakly influenced by the presence of carbon dioxide. Zhang et al. [40] considered a jet-stirred / plug-flow reactor. According to their numerical analyses, the effect of the addition of carbon dioxide is to raise the OH / H ratio, diminish the overall concentration of the O-H radical pool, and increase the availability of CO. This results in reduced concentrations of C_2H_2 and PAHs.

3. Modelling methodology

Unlike their gaseous precursors PAH, soot particles can be extremely diverse in terms of their precise number and the spatial arrangement of their atoms [15]. Consequently, the most detailed description of their growth usually consists of polymerisation processes accounted for through various mathematical methods [13, 31, 41]. While these approaches are suitable for simulating and numerically analysing soot formation and depletion in simplified systems such as shock tubes [15] or laminar flames [14], it is really hard to apply them to the Computational Fluid Dynamics (CFD) simulations of complex systems (such as car engines, incinerators or industrial burners) where the mere task of modelling the underlying gas-phase chemistry can already be computationally prohibitive [13]. Furthermore, even if a single CFD simulation of an industrial system based on a detailed or semi-detailed mechanism might be realisable with the help of a supercomputer, such simulations could not be performed under a wide variety of conditions, as would be necessary to reach a thorough understanding of the complex set of overlapping reactions and their interactions [33]. Consequently, in the frame of the present work, we decided to focus our attention on the chemical effects of CO_2 on soot formation by considering the *homogeneous* combustion of CH_4-CO_2 blends of diverse compositions in systems such as shock tubes or rapid compression machines where variables only depend on the reaction time. Proceeding in this way, we were able to isolate the *chemistry* from thermodynamical aspects that might be entangled with it otherwise [35, 38].

We further needed a way to qualify the sooting or aromatic tendency of a mixture at a given pressure and at a given temperature. We considered the *propensity to form soot* to be well represented by the mole fraction of benzene, the first aromatic ring.

$$Precursors(t) = X_{A1}(t)$$

whereby A_1 stands for benzene. In this work, we first defined the propensity of a *given set of conditions* (encompassing initial mole fractions, pressure, temperature, and reaction time) to bring about aromatic compounds and soot as the *maximum* of benzene mole fraction over the entire time period, that is to say

$$Soot_p = max\{X_{A1}(t), t \in [0; t_{end}]\}$$

This choice was motivated by the fact that PAH formation and PAH concentrations determine soot formation [42–45] to a great extent, that PAH peak concentrations are closely correlated to sooting limits and that the propensity of a flame to form soot is characterised by its propensity to form PAH [46]. Several experimental and theoretical studies have emphasised that the formation of soot and of PAH from aliphatic hydrocarbons (including, of course, CH_4 and mixture thereof with CO and CO_2) is highly dependent on the formation of benzene A_1 [12, 29, 30, 43, 47–50]. We tried to also consider aromatic species such as naphtalene (A_2), phenanthren (A_3), Acenaphthylen (A_2R_5) or Pyrene (A_4) and their sum, but this did not bring in any additional information relevant to our qualitative comparison. What is more, the very small values of some of these concentrations led to numerical problems and irregularities of the profiles. Consequently, the computation of benzene A_1 appears to be ideal in terms of representing the formation of aromatic compounds in CH_4 - CO_2 blends. Given the uncertainty of their coefficients [15, 31], describing the formation and growth of soot particles would have considerably increased the duration of our computations without bringing in any new reliable qualitative and quantitative information relevant to our concerns.

We considered four detailed reaction mechanisms describing the formation of PAH to perform our simulations:

- the model of Frenklach et al. [14, 51, 52] which was developed for describing soot formation during the combustion of small hydrocarbons. It was validated through comparisons with experimental profiles of major and minor chemical species, aromatic compounds, soot volume fractions, and soot particle diameters reported in the literature for nine laminar premixed flames of ethane, ethylene, and acetylene.

- the model of Li et al. [53] which aims at accounting for the combustion of toluene. It was tested against toluene-O_2-Ar premixed laminar flames over a broad range of equivalence ratios (Φ = 0.75 - 1.75) at low pressure. The species profiles encompass H_2, H_2O, CO, CO_2, small aliphatic hydrocarbons and small aromatic compounds.

- the model of Raj et al. [45] which describes the combustion of gasoline surrogate fuels (n-heptane, iso-octane and toluene). The mechanism has been validated for premixed laminar flames of n-heptane, iso-octane, benzene and ethylene. The measured profiles include H_2, H_2O, CO, CO_2, C_2H_2 and aromatic compounds from benzene (A_1) to coronene (A_7). Its prediction of PAH profiles follows the same trend as that of soot mole fractions in the counterflow flames of n-heptane/toluene and iso-octane/toluene mixtures.

- the model of Chernov et al. [54] that was designed in order to simulate the formation of soot and its precursors during the combustion of small aliphatic hydrocarbons ($C_1 - C_2$). It was validated with respect to the profiles of small hydrocarbons (such as C_2H_2) and aromatic compounds in methane/oxygen, C_2H_6-CO_2-Ar premixed flames and soot volume fractions in methane, ethane and ethylene co-flow flames.

We also used a partially reduced mechanism developed by Wang et al. [55] to simulate PAH and soot formation during the combustion of n-dodecane. It was validated through the ignition delay times of n-dodecane and n-decane in shock tubes, species profiles measured during the combustion of n-dodecane in a jet stirred reactor and shock tube (O_2, CO, CO_2, C_2H_2, C_2H_4, A_1) as well as soot volume fractions in n-dodecane spray flames.

As we want to predict the formation of aromatic species during the combustion of $CH_4 - CO_2$ blends, we first compared the performances of these five reaction mechanisms with respect to ignition delay times related to various mixtures involving methane, carbon monoxide and carbon dioxide. The simulations of the shock tube measurements have been carried out with the software Homrea [56–58] using homogeneous zero-dimensional assumptions involving a constant volume V and a constant internal energy U. For each experimental study we considered, we defined the modelled ignition delays in the same way the original authors had measured them (e.g. as corresponding to the peak concentration of OH or the greatest slope of $p(t)$). For a series of n measurements, we systematically calculated the *average logarithmic distance* between model and experiment $d(p)$

$$d(p) = \frac{\sum_{i=1}^{n} |log_{10}(\tau_{m,i}) - log_{10}(\tau_{e,i})|}{n}$$

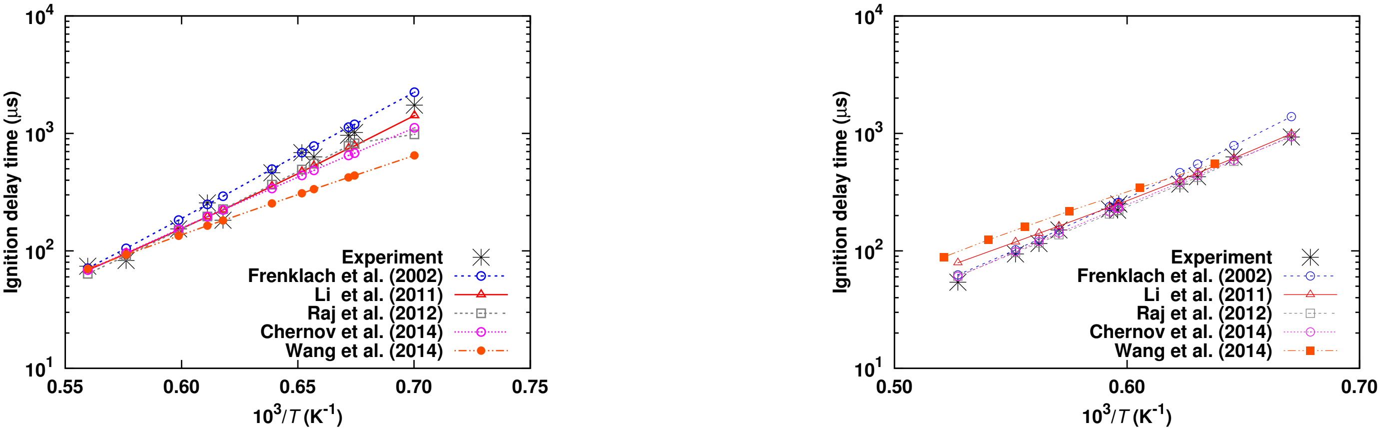

(a) Methane, first series

(b) Biogas, first series

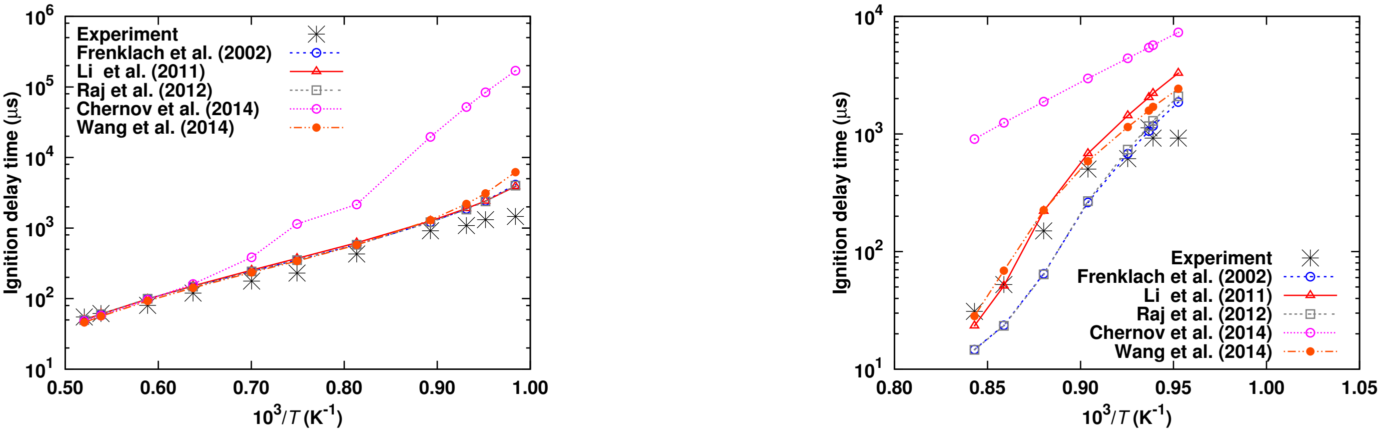

(c) Bio-syngas, first series

(d) CH_4- CO- CO_2 -H_2, first series

Figure 1: Experiments and model predictions

whereby $\tau_{m,i}$ and $\tau_{e,i}$ are the model prediction and the experimental measurement, respectively.

4. Test and comparison of the reaction mechanisms

To test and compare the reaction mechanisms, we considered experiments involving methane [59], biogas [60], bio-syngas [61] and various mixtures of CH_4, CO, CO_2, and H_2 [62]. Due to space limitation, we only summarised our results here. The reader is referred to **Supplementary material 1 - Model Evaluation** to see the experimental conditions, the detailed results and their interpretation. Figure 1 illustrates the results we obtained. Table 1 contains the values of the average discrepancies. It can be seen that the model of Li et al. [53], closely followed by that of Raj et al. [45], leads to the best average performance. For methane mixtures, the results of Li et al. ($d = 0.084$) are slightly better than those of Raj et al. ($d = 0.095$). For biogas mixtures, the predictions of Raj et al. ($d = 0.057$) are marginally superior to the ones of Li et al. ($d = 0.063$). For bio-syngas mixtures, Li et al. provides us with better results ($d = 0.181$) than Raj et al. ($d = 0.137$) . For CH_4 - CO_2 - CO - H_2 blends, the predictions of Li et al. ($d =$

Table 1: Average logarithmic discrepancies

Series	Frenklach et al.	Li et al.	Raj et al.	Chernov et al.	Wang et al.
Methane	0.129	0.084	0.095	0.098	0.216
Biogas	0.081	0.063	0.057	0.059	0.178
Bio-syngas	0.145	0.181	0.137	0.550	0.162
CH_4- CO- CO_2 -H_2	0.333	0.128	0.334	0.768	0.239
All	0.131	0.101	0.111	0.252	0.189

0.128) are largely superior to those of Raj et al. ($d = 0.334$).

We decided to use the mechanism of Li et al. for all our computations. Besides its modest superiority to that of Raj et al. in terms of predictions of the above measurements, it was specifically designed to simulate the pyrolysis and oxidation of toluene. It thus naturally includes many elementary steps describing the growth and oxidation of aromatic compounds. It also involves important reaction pathways responsible for the formation of the first aromatic rings during the combustion of aliphatic fuels, such as those involving the radicals propargyl C_3H_3 [43, 63–66] and cyclopentadienyl $c - C_5H_5$ [43, 67–69]. While the mechanism developed by Raj et al. presents many of the same advantages, it contains considerably more reactions, most of which accounting for the combustion of n-heptane and iso-octane. They would considerably raise the computational burden without playing any role in the burning of $CH_4 - CO_2$ and $CH_4 - CO$ mixtures.

5. Isothermal mixtures highly diluted in Argon

5.1. Numerical results

In order to decouple the chemical kinetics from the thermodynamics, we defined a series of **isothermal** trials highly diluted in Argon at atmospheric pressure. Since for any given equivalence ratio, the initial concentration of CH_4, O_2 and N_2 are the same, any differences in the temporal or temperature-dependent profiles of other species can only stem from the *participation of carbon dioxide in chemical reactions* which changes with its initial amount. In what follows, we considered three such equivalence ratios ($\phi = 1$, $\phi = 3$ and $\phi = 5$) and four fuels containing 0%, 25%, 50%, and 75% of CO_2. In order to have an overview of such effects, we first represented the temperature-dependent profiles of the variable $max\{X_{A1}(t), t \in [0; t_{end}]\}$ as illustrated in Figure 2 for a rich mixture ($\phi = 3$), whereby t_{end} = 20 s so as to systematically capture the highest values of benzene mole fractions. The highest values of $max(X_{A1})$ centres generally around a certain temperature T_{max} which equals **1350 K** for $\phi = 3$. Consequently, we decided to perform our comparisons by considering the *temporal profiles* of benzene A_1 computed at the T_{max} corresponding to each stoichiometry.

Different trials and errors we conducted showed us this is the optimal way to visualise the chemical effects of CO_2

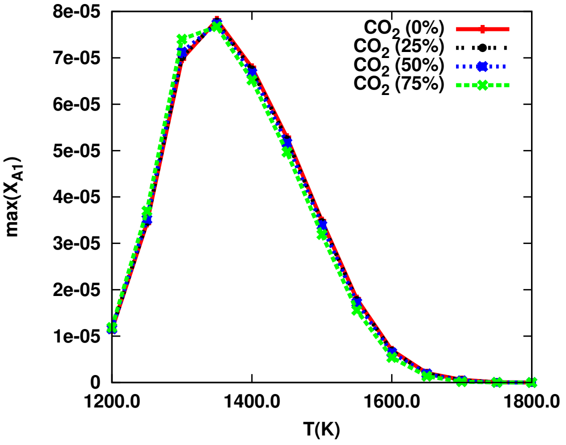

(a) $max(X_{A1}(t))$

Figure 2: A_1 formation for $\phi = 3$ under isothermal conditions

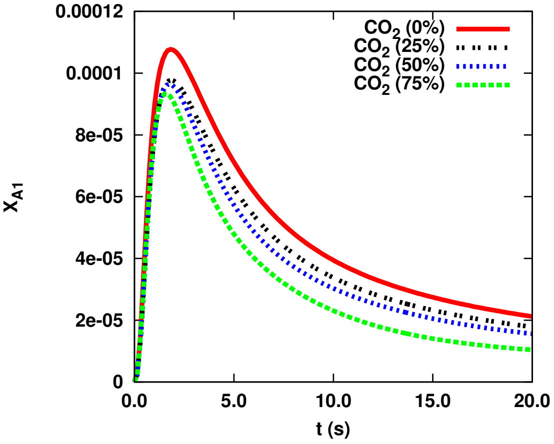

(a) X_{A1} at $T = 1450.0$ K

Figure 3: Time-dependent series for $\phi = 5$ at $p = 1$ atm and high dilution in Argon

addition on aromatic species, as they follow the same tendencies as benzene. It is important to always remember that *all computations included in our article* were performed at **atmospheric pressure** as this will not be repeated later on. Finally, it is noteworthy that the effect of CO_2 addition on the *maximum* mole fraction of benzene is scarcely noticeable for isothermal calculations, as can be clearly recognised in Figure 2. The temporal profile of benzene has been computed for $\phi = 5$ and is reported in Figure 3. Further results for $\phi = 1$ and $\phi = 3$ are described in **Supplementary material 2 - Additional results**. It is worth noting we obtained qualitatively similar results while performing simulations under lean conditions. We did not include them, however, because the very small concentrations of aromatic compounds make them prone to numerical errors, which results in unnatural discontinuities in the profiles.

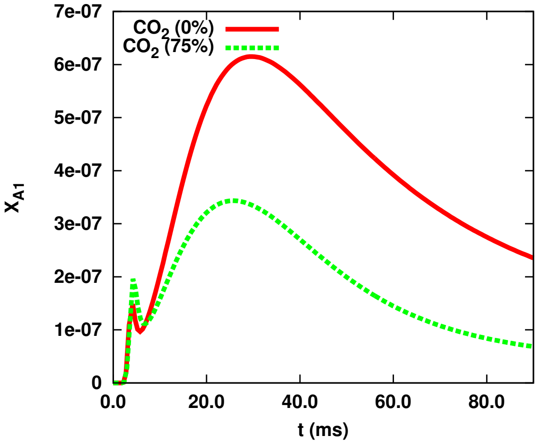

Figure 4: A_1 profiles for $\phi = 3$ and $T = 1700$ K and the same collision efficiencies for CO_2 and AR

5.2. Kinetics effects of CO_2 *addition on PAH formation*

As mentioned above, the isothermal conditions involving mixtures highly diluted in the inert gas Argon allow the chemical kinetics to completely govern the behaviour of the system. An analysis of the above results is following.

The formation of benzene is very weak under the stoichiometric combustion of methane with or without added carbon dioxide. While the highest mole fraction of A_1 remains approximately the same, increasing the initial abundance of CO_2 delays its formation (see **Supplementary material 2 - Additional results**). For very rich mixtures (Figure 3), the presence of additional carbon dioxide noticeably suppresses the formation of benzene. Thus, our numerical results strongly suggest that carbon dioxide addition has an inhibitive action on benzene which is purely chemical. This stands in contrast to studies mainly attributing this inhibition to thermal effects [33, 35, 38]. A possibility which must be considered is that while CO_2 does not take part in reactions as a reactant, it nonetheless influences the overall reactivity of the system because it does not have the same collision efficiencies in the definition of third bodies as Argon, nitrogen or other species. To evaluate the viability of this explanation, *we replaced the collision efficiencies of* CO_2 *by the values of AR* and compared the temporal profiles of benzene for $\phi = 3$ and $T = 1700$ K obtained with pure methane and a mixture of 25% of CH_4 and 75% of CO_2. The results are reported in Figure 4. It can be clearly recognised that the differences between both profiles remain considerable despite argon and carbon dioxide having the same collision efficiencies. Comparisons performed under similar conditions deliver the same type of results. This, in turn, clearly demonstrates that the reaction mechanism predicts the chemical participation of CO_2 to reactions impacting benzene formation and depletion.

5.3. Sensitivity analyses related to A_1

To further evaluate the conclusions drawn above, sensitivity analyses were conducted at T = 1350 K for $t = 90.0$ s where benzene is being consumed. The analyses were carried out with respect to pure methane and a blend containing 25% of methane and 75% of carbon dioxide as this yielded the greatest differences in terms of A_1 formation and depletion. The results are displayed in Figure 5. In both cases, the chemistry related to the propargyl radical C_3H_3 proved of great importance to the chemistry of benzene. The peak concentration of A_1 was shown to be sensitive to the reactions $CH_3 + C_2H_2 \rightleftharpoons H + PC_3H_4$, $CH_3 + PC_3H_4 \rightarrow CH_4 + C_3H_3$, $PC_3H_4 \rightarrow H + C_3H_3$, $H + PC_3H_4 \rightarrow H_2 + C_3H_3$, $H + C_3H_3 \rightarrow H_2 + C_3H_2$, and $AC_3H_4 \rightleftharpoons PC_3H_4$. Such a trend has been identified in various other studies [43, 63–66]. Unlike these works, the self-recombination of propargyl $C_3H_3 + C_3H_3 \rightarrow A_1$ was found to be considerably less important than $C_3H_3 + PC_3H_4 \rightarrow H + A_1$. The direct chemical action of carbon dioxide manifests itself through the reaction $H + CO_2 \rightleftharpoons OH + CO$ which, in both directions, plays a remarkable role in the CH_4 (25%) - CO_2 (75%) mixture, whereas its influence on benzene concentration is very small in the absence of CO_2 among the reactants. Furthermore, our results confirm the findings of Liu et al. [70] and Mancarella et al. [37], according to which the suppression of soot and PAH goes through an increase in the concentration of OH formed via $H + CO_2 \rightarrow OH + CO$, as the elementary steps $OH + A_1 \rightleftharpoons H_2O + A_1-$, $H_2O + CH_3 \rightarrow OH + CH_4$, $OH + A_1 \rightleftharpoons H + A_1OH$, and $OH + CH_4 \rightleftharpoons H_2O + CH_3$ involving the hydroxyl radical were all shown to significantly influence benzene concentration and have higher sensitivity coefficients under the presence of carbon dioxide.

6. Adiabatic combustion

6.1. Temperature-dependent profiles for $\phi = 3$

Here, the effects of CO_2 addition on the adiabatic combustion of methane undiluted in argon have been investigated. The initial mole fraction of methane always equals 15% whereas the concentration of carbon dioxide and oxygen are varied according to the amount of CO_2 and the equivalence ratio, respectively. The rest of the reactive mixture is constituted of N_2 in the absence of argon.

First, the temperature-dependent profile of $max(X_{A1})$ has been represented at an equivalence ratio of $\phi = 3$. The initial conditions of the adiabatic computations are given in Table 2. It has been contrasted with the isothermal results of section 5 also obtained for $\phi = 3$. The results are shown in Figure 6.

A paradoxical effect emerges out of these data. For our isothermal and kinetically-controlled simulations, CO_2 addition has nearly no effect on the peak concentration of benzene as function of the temperature (and as we saw, it leads to its kinetic suppression while considering temporal profiles). Yet, at the same time, CO_2 addition under

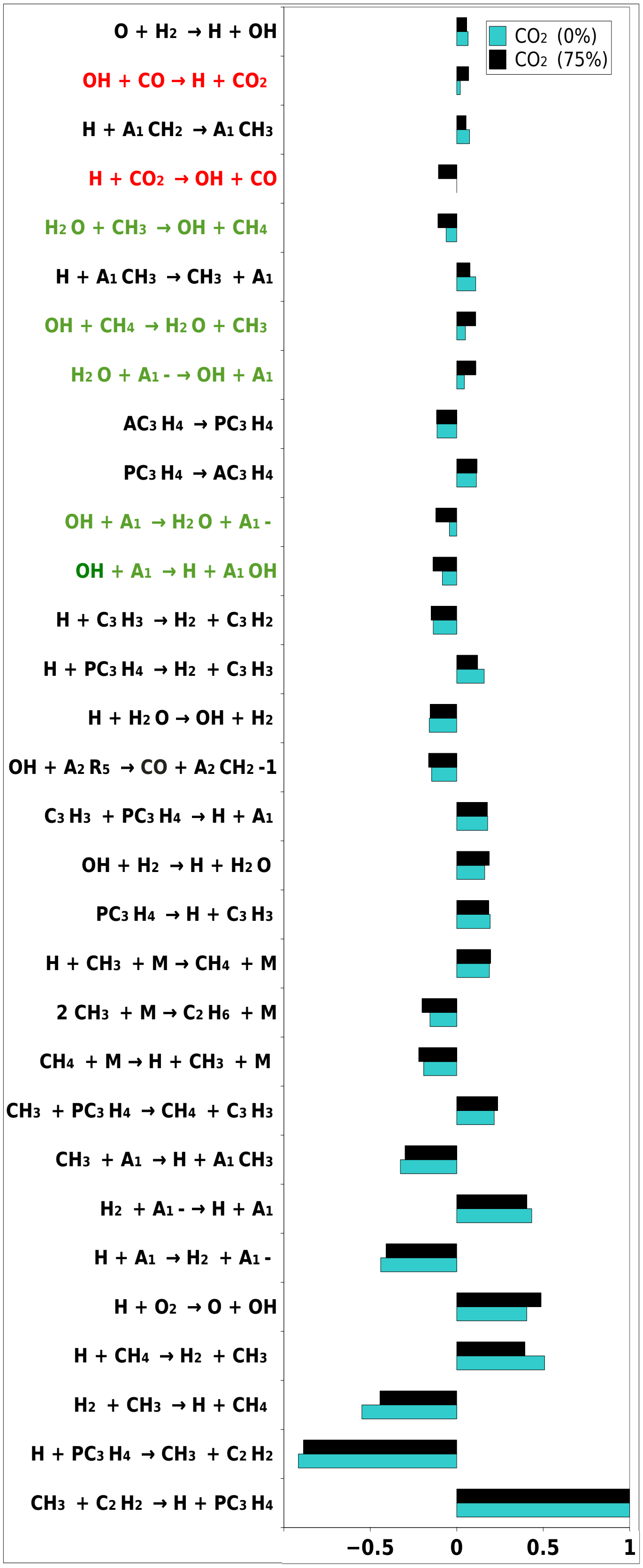

Figure 5: Reaction sensitivity analysis under isothermal conditions

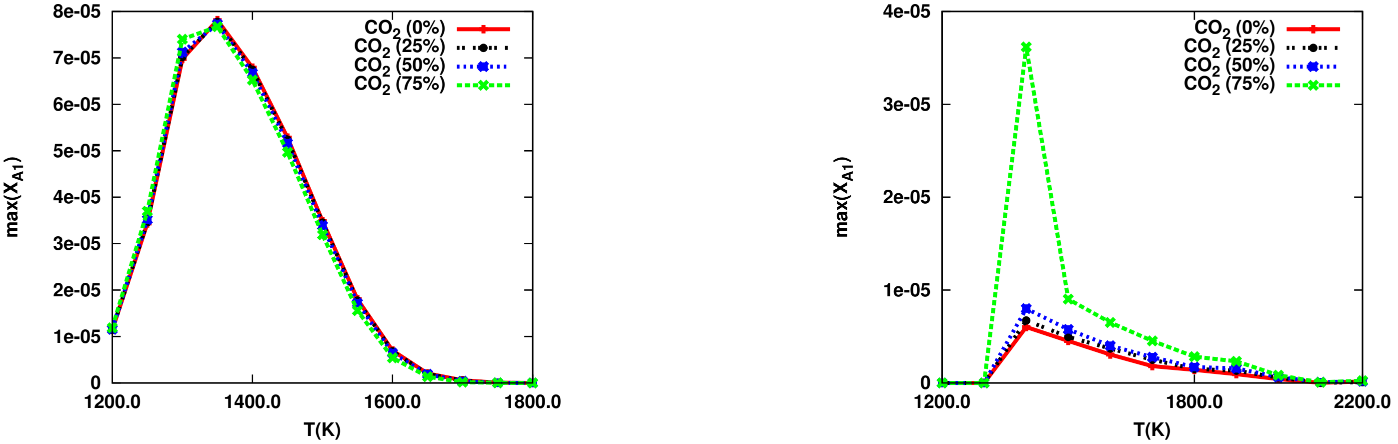

(a) A_1, isothermal

(b) A_1, adiabatic

Figure 6: Comparison between isothermal and adiabatic simulations for $\phi = 3$

adiabatic conditions leads to an **increase** in the highest mole fraction of A_1. The maximum concentration of benzene produced under the presence of 75% of carbon dioxide in the fuel even exceeds that produced in the absence of CO_2 by a factor of 7. To understand the causes of this highly counter-intuitive result, the temporal adiabatic profiles of X_{A1}, X_{OH} and $T(t)$ have been computed for $\phi = 3$ in section .

6.2. Adiabatic time-dependent profiles for $\phi = 3$

The temporal profiles of the mole fractions of benzene and the hydroxyl radical and of the temperature have been computed, based on the conditions of Table 2. They are reported in Figure 10. Considering simultaneously the evolution of these variables helps explain the peculiar trend discovered above. The presence of a large proportion of CO_2 among the reactants goes hand in hand with an overall diminution of the temperature, which does not increase as strongly as in the absence of carbon dioxide in the fuel. This, in turn, is correlated with a considerably smaller peak concentration of OH which consequently cannot potently oxidise A_1 and its precursors.

6.3. Adiabatic combustion without the kinetics of CO_2

In order to increase our understanding of these phenomena, we carried out the same simulations as in section 5 but without any reactions involving carbon dioxide *as a reactant*. The modifications are reported in **Supplementary**

Table 2: Mole fractions of series 3 (Adiabatic)

CO_2 in Biogas	X_{CH4}	X_{CO2}	X_{O2}	X_{N2}
0.0%	0.15	0.00	0.10	0.75
25.0%	0.15	0.05	0.10	0.70
50.0%	0.15	0.15	0.10	0.60
75.0%	0.15	0.45	0.10	0.30

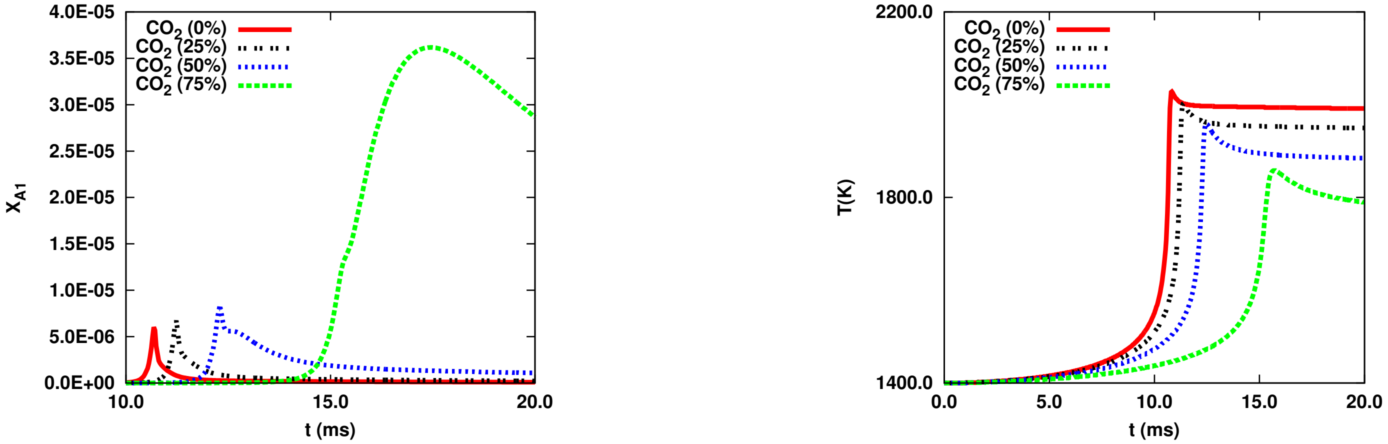

(a) X_{A1} at $T_0 = 1400.0$ K

(b) $T(t)$ at $T_0 = 1400.0$ K

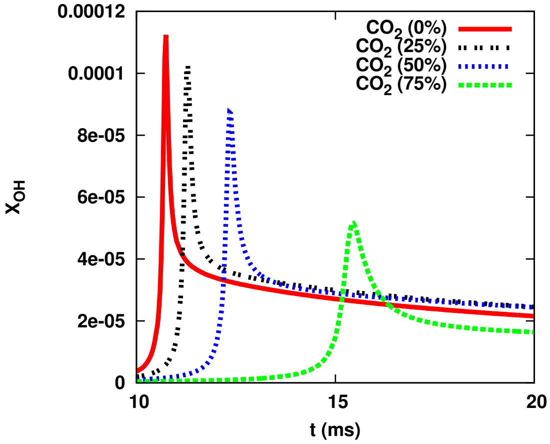

(c) X_{OH} at $T_0 = 1400.0$ K

Figure 7: Time-dependent series for $\phi = 3$ at $p = 1$ atm under adiabatic conditions

material 3 - Reactions with CO_2. Using the conditions of Table 2, we computed the temperature-dependent evolution of $max(X_{A1})$ without CO_2-kinetics for $\phi = 3$ and $p = 1$ atm under adiabatic conditions. The results are shown in Figure 8, where they are contrasted with those obtained in Figure 6. Moreover, the temporal profile of the mole fractions of benzene has been computed in the absence of reactions involving CO_2 as a reactant, based on the conditions of Table 2, that is $\phi = 3$, $p = 1$ atm and $T_0 = 1400$ K under adiabatic conditions. It is displayed in Figure 9. Whilst the deactivation does not affect the profile of benzene during the combustion of pure methane and $CH_4(75\%) - CO_2(25\%)$ blend, it results in a very strong increase of A_1 mole fraction if the fuel contains 75% of carbon dioxide. This suggests that, under adiabatic conditions, these chemical reactions enhance benzene formation instead of inhibiting it as they do under isothermal conditions.

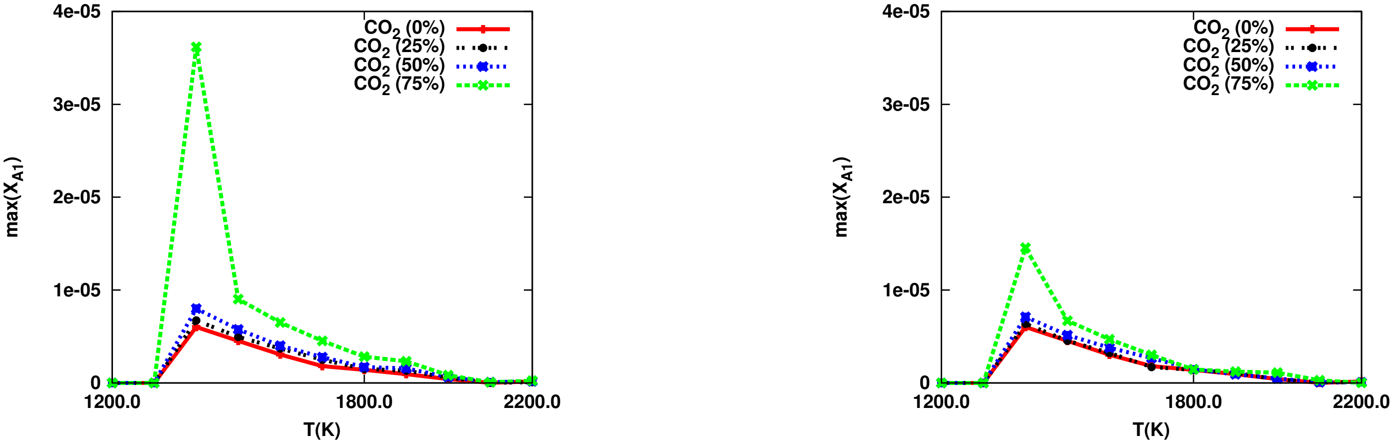

(a) X_{A1} with CO_2-kinetics

(b) X_{A1} without CO_2-kinetics

Figure 8: Adiabatic combustion with and without CO_2-kinetics

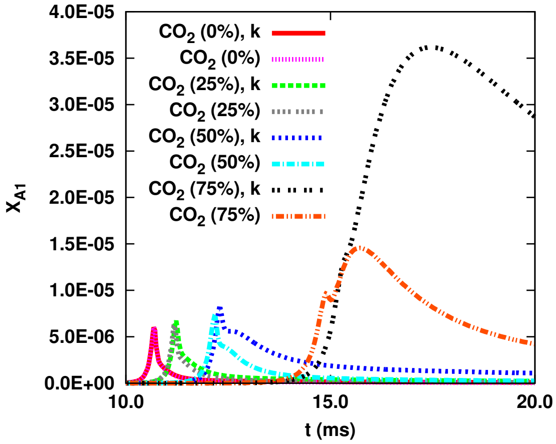

Figure 9: Temporal profile of X_{A1} with and without CO_2-kinetics

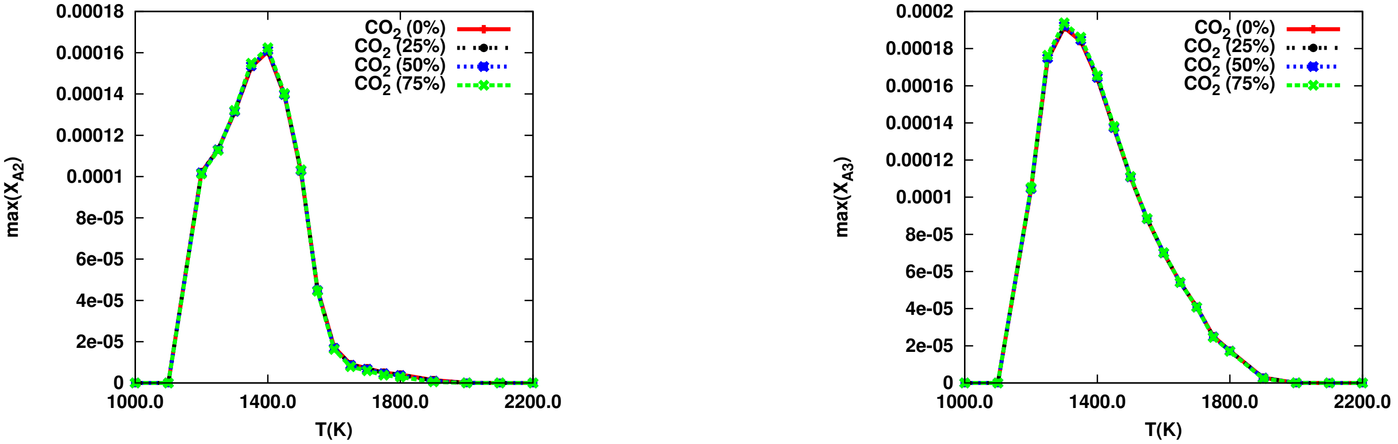

(a) $max(X_{A2}(t))$

(b) $max(X_{A3}(t))$

Figure 10: Combustion of A_1-CO_2 blends for $\phi = 3$

7. Chemical effects of CO_2 addition to A_1

In spite of all our efforts, we could not find any studies considering the effects of CO_2-addition to benzene during the combustion of the latter. Rosso et al. [71] investigated the reaction of carbon dioxide radical anion with substituted benzenes in aqueous solutions. There does not appear to be any direct connections between their results and our main concerns in this article. Consequently, we considered it worthwhile to perform a chemical-kinetic isotherm studies of the effects of CO_2-addition to benzene while using conditions closely similar to those of section 5. The highest mole fractions of naphtalene A_2 and phenanthrene A_3 have been represented as function of the temperature, for $\Phi = 3$, in Figure 10. The addition of carbon dioxide to benzene does not cause any noticeable differences to the chemistry of growing aromatic compounds ultimately leading to soot. The same observation was made while producing similar curves for $\phi = 1$ and $\phi = 5$. The temporal profiles of A_2, A_3, A_4, OH, H and CO have been computed for $\phi = 3$ at $T =$ 1400 K where the concentrations of the aromatic species reach high values. The results (shown in **Supplementary material 2 - Additional results**) confirm that the changes in all these profiles are barely noticeable.

The main result of this section is that the addition of carbon dioxide to benzene (and probably also to higher aromatic compounds) has either a very weak or a non-existent influence on the combustion chemistry *if thermodynamic effects do not occur*, i.e. the temperature remains constant. As a consequence, during the combustion of biogas, the direct chemical action of carbon dioxide involves reactions preceding the formation of the first aromatic ring, at the level of small aliphatic hydrocarbons and their radicals.

8. Conclusion and outlook

The goal of the present article was to increase our understanding of the formation of the first aromatic species (represented by benzene) through chemical reactions CO_2 takes part in. In Section 5, we investigated the *purely chemical* effects of carbon dioxide addition to methane by performing isothermal simulations involving various CO_2 amounts and equivalence ratios. We found that increasing the concentration of carbon dioxide reduces the concentration of benzene. This effect seems to be due to a growth in the concentration of the oxidising radical OH via the step $CO_2 + H \rightarrow CO + OH$. In section 6, we investigated CO_2 addition under adiabatic conditions. We identified a very peculiar phenomenon: while higher initial concentrations of carbon dioxide under isothermal conditions chemically inhibit the formation of benzene, they *greatly increase* it under adiabatic conditions. We could show this is caused by CO_2 thermally inhibiting the whole combustion, thereby leading to lower levels of OH radicals which cannot oxidise benzene and its precursors as efficiently as when pure methane is burnt. Even more unexpected was our discovery of the two natures of the role plaid by reactions involving CO_2 as reactants (such as $CO_2 + OH \rightarrow CO + HO_2$ or $CO_2 + H \rightarrow CO + OH$). While they reduce the concentration of benzene under isothermal conditions, they increase it under adiabatic conditions. Eventually, in Section 7, we found that the direct addition of CO_2 to benzene does not cause any significant differences in the profiles of aromatic species and small radicals. Thus, during the combustion of biogas, CO_2 can only chemically participate in reactions with smaller aliphatic hydrocarbons and radicals which precede steps involving aromatic compounds.

While we mainly presented results related to benzene, our computations showed us that the same trends can be observed for higher aromatic species. These, in turn, determine the sooting behaviour of any flames [26–29]. Whilst we had interesting and unexpected results, our study was numerical and qualitative. As a consequence, we believe future kinetic experiments under conditions close to those we considered could prove extremely valuable. Besides confirming or mitigating the conclusions we drew, they would also provide experimental information for the estimation and optimisation of kinetic parameters. For example, isothermal experiments entirely controlled by chemical kinetics (such as simulated in Section 5) could be performed in flow reactors where the effects of mass diffusion and wall surface reactions can be neglected or accurately assessed [72, 73]. Undiluted adiabatic experiments could, for instance, be conducted in shock tubes where the assumptions of constant volume and constant energy remain approximately valid during the measurements of the profiles [74–76]. We believe that such experiments could prove very valuable to applied scientists and practitioners alike who are interested in assessing the complex consequences of using biogas, both in specific situations and on a global scale.

References

[1] McManus MC, Taylor CM. The changing nature of life cycle assessment. Biomass and Bioenergy 2015;82:13–26.

[2] McManus MC, Taylor CM, Mohr A, Whittaker C, Scown CD, Borrion AL, Glithero NJ, Yin Y. Challenge clusters facing lca in environmental decision-makingwhat we can learn from biofuels. International Journal of Life Cycle Assessment 2015;20:1399–1414.

[3] Budzianowski WM. A review of potential innovations for production, conditioning and utilization of biogas with multiple-criteria assessment. Renewable and Sustainable Energy Reviews 2016;54:1148–1171.

[4] Ding M, Tu J, Zhang Q, Wang M, Tsubaki N, Wang T, Ma L. Enhancement of methanation of bio-syngas over CeO_2-modified Ni / Al_2O_3 catalysts. Biomass and Bioenergy 2016;85:12–17.

[5] Moreira N. Biomethane as a substitute for natural gas. Digestion 2016;20:7.

[6] Rasi S, Veijanen S, Rintala J. Trace compounds of biogas from different biogas production plants. Energy 2007; 32:1375–1380.

[7] Hegarty M, O'Connor A, Ross J. Syngas production from natural gas using ZrO_2-supported metals. Catalysis Today 1998;42:225–232.

[8] Robbins M, Evans G, Valentine J, Donnison I, Allison G. New opportunities for the exploitation of energy crops by thermochemical conversion in the UK . Progress in Energy and Combustion Science 2012;38:138–155.

[9] Fischer M, Jiang X. An assessment of chemical kinetics for bio-syngas combustion. Fuel 2014;137:293–305.

[10] Fischer M, Jiang X. An investigation of the chemical kinetics of biogas combustion. Fuel 2015;150:711–720.

[11] Fischer M, Jiang X. A chemical kinetic modelling study of the combustion of CH_4 - CO - H_2 - CO_2 fuel mixtures. Combustion and Flame 2016;167:274–293.

[12] Mansurov ZA. Soot formation in combustion processes. Combustion, Explosion, and Shock Waves 2005;41:727–744.

[13] Marquetand J, Fischer M, Naydenova I, Riedel U. A simplified model for soot formation in gas turbine combustion chambers. Fluid Mechanics and Its Applications 2012;1581:205–233.

[14] Frenklach M. Reaction mechanism of soot formation in flames. Phys Chem Chem Phys 2002;4:2028–2037.

[15] Naydenova I. Soot formation modeling during hydrocarbon pyrolysis and oxidation behind shock waves. Ph.D. thesis, Ruprecht-Karls-Universitt Heidelberg 2007.

[16] Cheung SC, Yuen RK, Yeoh GH, Cheng GW. Contribution of soot particles on global radiative heat transfer in a two-compartment fire. Fire Safety Journal 2004;39:412–428.

[17] Schnelle-Kreis J, Gebefgi I, Welzl G, Jaensch T, Kettrup A. Occurrence of particle-associated polycyclic aromatic compounds in ambient air of the city of munich. Atmospheric Environment 2001;35:S71–S81.

[18] Oberdorster G. Lung particle overload: implications for occupational exposures to particles. Regulatory Toxicology and Pharmacology 1995;21:123–135.

[19] Kennedy IM. The health effects of combustion-generated aerosols. Proceedings of the Combustion Institute 2007; 31:2757–2770.

[20] Zhiqiang Q, Siegmann K, Keller A, Matter U, Scherrer L, Siegmann HC. Nanoparticle air pollution in major cities and its origin. Atmospheric Environment 2000;34:443–451.

[21] Whittaker A, BeruBe K, Jones T, Maynard R, Richards R. Killer smog of london, 50 years on: particle properties and oxidative capacity. Science of the Total environment 2004;334:435–445.

[22] Ramanathan V, Carmichael G. Global and regional climate changes due to black carbon. Nature geoscience 2008; 1:221–227.

[23] Bekki S. On the possible role of aircraft-generated soot in the middle latitude ozone depletion. Journal of Geophysical Research 1997;102:751.

[24] Krestinin AV, Kislov MB, Raevskii AV, Kolesova OI, Stesik LN. On the mechanism of soot particle formation. Kinetics and Catalysis 2000;41:90–98.

[25] Richter H, Granata S, Green W, Howard J. Detailed modeling of PAH and soot formation in a laminar premixed benzene/oxygen/argon low-pressure flame. Proceedings of the Combustion Institute 2005;30:1397–1405.

[26] Balthasar M, Frenklach M. Detailed kinetic modeling of soot aggregate formation in laminar premixed flames. Combustion and Flame 2005;140:130–145.

[27] Singh J, Balthasar M, Kraft M, Wagner W. Stochastic modeling of soot particle size and age distributions in laminar premixed flames. Proceedings of the Combustion Institute 2005;30:1457–1465.

[28] Mitchell P, Frenklach M. Particle aggregation with simultaneous surface growth. Phys Rev E 67, 061407 2003; 67.

[29] Oektem B, Tolocka MP, Zhao B, Wang H Johnston MV. Chemical species associated with the early stage of soot growth in a laminar premixed ethylene–oxygen–argon flames. Combustion and Flame 2005;142:364–373.

[30] McEnally C, Pfefferle L. The effects of dimethyl ether and ethanol on benzene and soot formation in ethylene nonpremixed flames. Proceedings of the Combustion Institute 2007;31:603–610.

[31] Bockhorn H. Soot formation in combustion: mechanisms and models. Springer Science & Business Media, 2013.

[32] Samanta A, Ganguly R, Datta A. Effect of CO2 Dilution on Flame Structure and Soot and NO Formations in CH4-Air Nonpremixed Flames. J Eng Gas Turbines Power 2010;132:124501–124501.

[33] Charest MR, Guelder OL, Groth CP. Numerical and experimental study of soot formation in laminar diffusion flames burning simulated biogas fuels at elevated pressures. Combustion and flame 2014;161:2678–2691.

[34] Berhan S, Atreya A, M C, Sacksteder K. Effect of Fuel Dilution by CO2 on Spherical Diffusion Flames in Microgravity. 39th AIAA Aerospace Sciences Meeting & Exhibit 2001;:1–9.

[35] Kailasanathan A, Yelverton T, Roberts W. Effect of diluents on soot precursor formation and temperature in ethylene laminar diffusion flames. Combustion and Flame 2013;160:656–670.

[36] Liu F, Guo H, Smallwood G, Gulder O. The chemical effects of carbon dioxide as an additive in an ethylene diffusion flame: implications for soot and NOx formation. Combustion and Flame 2001;125:778–787.

[37] Mancarella S, Sully A, Derudi M, Rota R, Granata S, Faravelli T, Ranzi E. Chemical and thermal effects of CO2 addition in fuel-rich premixed ethylene flames. Chemical Engineering Transactions 2007;11:1–6.

[38] Annunziata I, Sirignano M, DAnna A. The effect of carbon dioxide addition on soot formation in non-premixed ethylene flames. XXXV Meeting of the Italian Section of the Combustion Institute 2012;:1–7.

[39] Guo H, Smallwood G. A Numerical Study on the Influence of CO2 Addition on Soot Formation in an Ethylene/Air Diffusion Flame. Combustion Science and Technology 2008;180:10–11.

[40] Zhang Y, Lou C, Liu D, Li Y, Ruan L. Chemical Effects of CO2 Concentration on Soot Formation in Jet-stirred/Plug-flow Reactor. Chinese Journal of Chemical Engineering 2013;21:1269–1283.

[41] Chung S. Computational Modeling of Soot Nucleation. Ph.D. thesis, University of Michigan 2011.

[42] Kern R, Singh H, Wu C. Thermal combustion of 1,2butadiene. International Journal of Chemical Kinetics 1988; 20:731–747.

[43] DAnna A, Violi A, DAlessio A. Modeling the rich combustion of aliphatic hydrocarbons. Combustion and Flame 2000;121:418–429.

[44] Skjoeth-Rasmussen M, Glarborg P, Oestberg M, Johannessen J, Livbjerg H, Jensen A, Christensen T. Formation of polycyclic aromatic hydrocarbons and soot in fuel-rich oxidation of methane in a laminar flow reactor. Combustion and Flame 2004;136:91–128.

[45] Raj A, Prada I, Amer A, Chung S. A reaction mechanism for gasoline surrogate fuels for large polycyclic aromatic hydrocarbons. Combustion and Flame 2012;159:500–515.

[46] Kumfer B, Skeen S, Chen R, Axelbaum R. Measurement and analysis of soot inception limits of oxygen-enriched coflow flames. Combustion and Flame 2006;147:233–242.

[47] Richter H, Howard JB. Formation of polycyclic aromatic hydrocarbons and their growth to soot - a review of chemical reaction pathways. Progress in Energy and Combustion Science 2000;26:565–608.

[48] Agafonov G, Smirnov V, Vlasov P. Shock tube and modeling study of soot formation during the pyrolysis and oxidation of a number of aliphatic and aromatic hydrocarbons. Proceedings of the Combustion Institute 2011; 33:625–632.

[49] Dworkina S, Zhang Q, Thomson MJ, Slavinskaya NA, Riedel U. Application of an enhanced PAH growth model to soot formation in a laminar coflow ethylene/air diffusion flame. Combustion and Flame 2011;158:1682–1695.

[50] Oltena N, Senkan S. Formation of polycyclic aromatic hydrocarbons in an atmospheric pressure ethylene diffusion flame. Combustion and Flame 1999;118:500–507.

[51] Appel J, Bockhorn H, Frenklach M. Kinetic modeling of soot formation with detailed chemistry and physics: Laminar premixed flames of C2 hydrocarbons. Combustion and flame 2000;121:122–136.

[52] Wang H, Frenklach M. PAH formation and growth in laminar premixed ethylene and acetylene flames. Combustion and Flame 1997;110:173–221.

[53] Li Y, Cai J, Zhang L, Yuan T, Zhang K, Qi F. Investigation on chemical structures of premixed toluene flames at low pressure. Proceedings of the Combustion Institute 2011;1:593–600.

[54] Chernov V, Thomson M, Dworkin S, Slavinskaya N, Riedel U. Soot formation with C1 and C2 fuels using an improved chemical mechanism for PAH growth. Combustion and Flame 2014;161:592–601.

[55] Wang H, Ra Y, Jia M, Reitz R. Development of a reduced n-dodecane-PAH mechanism and its application for n-dodecane soot predictions. Fuel 2014;136:25–36.

[56] Warnatz J, Maas U, Dibble R. Combustion: Physical and Chemical Fundamentals, Modeling and Simulation, Experiments, Pollutant Formation. Springer, 2006, Springer Science & Business Media edition.

[57] Norinaga K, Deutschmann O. Detailed kinetic modeling of gas-phase reactions in the chemical vapor deposition of carbon from light hydrocarbons. Ind Eng Chem Res 2007;46:3547–3557.

[58] Khan R, Buchholz D, Graf F, Reimert R. Pyrolysis of acetylene for vacuum carburizing of steel: Modeling with detailed kinetics. International Journal of Chemical Reactor Engineering 2009;7:1542.

[59] Seery D, Bowman C. An experimental and analytical study of methane oxidation behind shock waves. Combustion and Flame 1970;14:37–47.

[60] Zeng W, Hongan M, Liang Y, Hu E. Experimental and modeling study on effects of N2 and CO2 on ignition characteristics of methane/air mixture. Journal of Advanced Research 2015;6:189–201.

[61] Mathieu O, Kopp M, Petersen E. Shock-tube study of the ignition of multi-component syngas mixtures with and without ammonia impurities. Proceedings of the Combustion Institute 2013;34:3211–3218.

[62] Kalitan D. A study of syngas oxidation at high pressures and low temperatures. Ph.D. thesis, University of Central Florida 2007.

[63] Dias V, Renard C, Van Tiggelen P, Vandooren J. Modeling of soot precursors in rich premixed ethylene/oxygen/argon flames. Proceedings of the European Combustion Meeting 2003;1:1–6.

[64] McEnally C, Pfefferle L, Atakan B, Kohse-Hoeinghaus K. Studies of aromatic hydrocarbon formation mechanisms in flames: Progress towards closing the fuel gap. Progress in Energy and Combustion Science 2006;32:247–294.

[65] Guo H, Trottier S, Johnson M, Smallwood G. A numerical investigation on soot formation from laminar diffusion flames of ethylene/methane mixture. ASME Heat Transfer Summer Conference collocated with the Fluids Engineering, Energy Sustainability, and 3rd Energy Nanotechnology Conferences 2008;3:1–7.

[66] Marinov M, Pitz W, Westbrook C, Vincitore A, Castaldi M, Senkan S, Melius C. Aromatic and polycyclic aromatic hydrocarbon formation in a laminar premixed n-butane flame. Combustion and Flame 1998;114:192–213.

[67] Boehm H, Jander H. PAH formation in acetylenebenzene pyrolysis. Phys Chem Chem Phys 1999;1:3775–3781.

[68] D'Anna A, Violi A. A kinetic model for the formation of aromatic hydrocarbons in premixed laminar flames. Symposium (International) on Combustion 1998;27:425–433.

[69] Kislov VV, Mebel AM. An Ab Initio G3-Type-Statistical Theory Study of the Formation of Indene in Combustion Flames. II. The Pathways Originating from Reactions of Cyclic C5 Species Cyclopentadiene and Cyclopentadienyl Radicals. J Phys Chem A 2008;112:700–716.

[70] Liu F, Guo H, Smallwood G. The chemical effect of CO2 replacement of N2 in air on the burning velocity of CH4 and H2 premixed flames. Combustion and Flame 2003;133:495–497.

[71] Rosso J, Bertolotti S, Braun A, Martire D, Gonzalez MC. Reactions of carbon dioxide radical anion with substituted benzene. J Phys Org Chem 2001;14:300–309.

[72] Lee J, Yetter R, Dryer F, Tomboulides A, Orszag S. Simulation and analysis of laminar flow reactors. Combustion Science and Technology 2000;159:199–212.

[73] Mehl M, Frassoldati A, Fietzek R, Faravelli T, Pitz W, Ranzi E. Chemical kinetic study of the oxidation of toluene and related cyclic compounds. Fall Technical Meeting of the Western States Section of the Combustion Institute, 2009, pp. 3 – 21.

[74] Davidson DF, Hanson RK. Interpreting shock tube ignition data. International Journal of Chemical Kinetics 2004;36:510–523.

[75] Tang W, Zhang L, Linninger AA Tranter R, Brezinsky K. Solving Kinetic Inversion Problems via a Physically Bounded Gauss-Newton (PGN) Method. Ind Eng Chem Res 2005;44:3626–3637.

[76] Mosbach S, Hong J, Brownbridge G, Kraft M, Gudiyella S, Brezinsky K. Bayesian error propagation for a kinetic model of n-propylbenzene oxidation in a shock tube. Int J Chem Kinet 2014;46:389 –404.